CANADA

DEPARTMENT OF
ENERGY, MINES AND RESOURCES
MINES BRANCH
OTTAWA

PILLAR LOADING
PART IV: INCLINED WORKINGS

D. F. COATES

FUELS AND MINING PRACTICE DIVISION

DECEMBER 1966

1867 1967

Research Report R 193 Price 75 cents

Available by mail from the Queen's Printer, Ottawa,
and at the following Canadian Government bookshops:

OTTAWA
Daly Building, Corner Mackenzie and Rideau

TORONTO
221 Yonge Street

MONTREAL
Æterna-Vie Building, 1182 St. Catherine St. West

WINNIPEG
Mall Center Building, 499 Portage Avenue

VANCOUVER
657 Granville Avenue

HALIFAX
1737 Barrington Street

or through your bookseller

A deposit copy of this publication is also available
for reference in public libraries across Canada

Price 25 cents Catalogue No. M38-1/193

Price subject to change without notice

ROGER DUHAMEL, F.R.S.C.
Queen's Printer and Controller of Stationery
Ottawa, Canada
1967

PREFACE

One of our major projects over the past few years has been the development of an hypothesis for predicting the loading of pillars. The progress of the project has been described in the following reports:

Pillar Loading. Part I: Literature Survey and New Hypothesis. (Mines Branch Research Report R 168, 1965)

Pillar Loading. Part II: Model Studies. (Mines Branch Research Report R 170, 1965)

Pillar Loading. Part III: Field Measurements. (Mines Branch Research Report R 180, 1966)

These reports describe how the objective of this work was substantially realized.

At the same time, it was assumed that the hypothesis would apply not only when the principal stresses in the formation are perpendicular and parallel to the plane of the orebody, but also when they were inclined to the orebody. It was decided that some experimental substantiation for this assumption was desirable. Thus the series of three reports has now been expanded into four to include the present report on inclined workings.

D.F. Coates

Mining Research Laboratories,
Ottawa, December 1966.

Mines Branch Research Report R 193

PILLAR LOADING. Part IV: Inclined Workings

by

D. F. Coates *

- - -

ABSTRACT

The new hypothesis that was recently developed for the determination of pillar loads was subsequently modified in the light of extensive experimental work. The resulting equations include significant factors not contained in the older tributary area theory. In this way, an improved basis is provided for predicting pillar loads.

In the new theory, and also in the experimental work, it was assumed that the principal stresses in the formation were perpendicular and parallel to the plane of the orebody. It was implied that when the principal field stresses were inclined to the plane of the orebody, the theory could still be used by only taking into account the components perpendicular and parallel to this plane. However, experimental substantiation of this assumption was required.

The work described in this report includes an examination of the theoretical implications of having the principal field stresses inclined to the plane of the orebody, and also includes measurements on models for these cases. The rigorous solution of the closure of an elliptical opening from the theory of elasticity is identical with the solution that would be obtained from the pillar loading hypothesis. In addition, the experimental work on model pillars showed good agreement with the predicted values obtained from the equations provided by the new theory.

The main conclusion from this work is that the use, in the previously reported derived equations, of only the components of principal field stresses perpendicular and parallel to the plane of an orebody has been substantiated as valid for the determination of pillar loading.

---

* Head, Mining Research Laboratories, Fuels and Mining Practice Division, Mines Branch, Department of Energy, Mines and Resources, Ottawa, Canada.

Direction des mines

Rapport de recherches R 193

LA CHARGE DES PILIERS. PARTIE IV: ABATTAGE INCLINÉ

par

D. F. Coates*

- - - -

RÉSUMÉ

La nouvelle hypothèse qui a récemment été élaborée pour déterminer la charge des piliers a été modifiée par la suite à la lumière de travaux expérimentaux considérables. Les équations qui en découlent comprennent d'importants facteurs dont on ne tenait pas compte dans l'ancienne théorie des zones tributaires. Nous disposons désormais d'une meilleure base pour déterminer les charges des piliers.

Dans la nouvelle théorie ainsi que dans les travaux expérimentaux, on a pris pour acquis que les contraintes principales dans la formation étaient perpendiculaires et parallèles au plan du gisement. Il était sous-entendu que lorsque les principales contraintes du terrain étaient obliques au plan du gisement, la théorie pourrait encore être utilisée en ne tenant compte que des contraintes perpendiculaires et parallèles à ce plan. Il fallait toutefois prouver expérimentalement le bien-fondé de cette hypothèse.

L'auteur étudie aussi les implications théoriques des cas où les contraintes principales du terrain s'exercent obliquement au plan du massif, et décrit aussi les mesures effectuées sur des modèles pour des cas semblables. La solution exacte de la fermeture d'une ouverture elliptique selon la théorie de l'élasticité est identique à la solution obtenue à partir de l'hypothèse de la charge des piliers. En outre, les travaux expérimentaux effectués sur des modèles de piliers ont bien confirmé les valeurs obtenues à l'aide des équations fournies par la nouvelle théorie.

La principale conclusion de ces travaux est qu'on a démontré la validité, dans la détermination de la charge des piliers, de l'utilisation, dans les équations dérivées déjà mentionnées, des seules composantes des contraintes principales du terrain perpendiculaires et parallèles au plan d'un gisement.

---

*Chef, Laboratoires de recherche en génie minier, Division des combustibles et du génie minier, Direction des mines, ministère de l'Énergie, des Mines et des Ressources, Ottawa, Canada.

CONTENTS

FIGURES

TABLES

INTRODUCTION

A new hypothesis was recently developed for the determination of pillar loads (1).* The resultant equations included such factors as the span of the mining zone, the height and breadth of the pillar, the position of the pillar in the mining zone, the variation between the deformability of the pillar and that of the wall rocks, and the effects on both the normal and transverse field stresses--all of which are not contained in the older tributary area theory. Consequently, the hypothesis has been shown to provide an improved basis for predicting pillar loads.

The new theory is based on the relation between the stress in a pillar and the deflection of the adjacent walls, this deflection being equal to that of the pillar. Through analysis of various components of the deflection of the walls as a result of mining, the resultant stresses in the pillars can be predicted.

The derivation was made for the cases which can be approximated by the assumption of plane strain (see Figure 1), i.e., where the mining zone is very long in the direction perpendicular to the span, and where one of the principal field stresses, S_o, is perpendicular to the orebody as shown in Figure 1. Experimental data obtained from various series of models by different workers substantiated the validity of the mechanisms included in the hypothesis (2). However, it was found necessary to modify the equations empirically to take into account the effects of mechanisms not explicitly included. The resultant agreement of the predictions with the results from the various model studies was then very good.

The equations developed from the theoretical and model work are as follows: (2)

$$\therefore \frac{\Delta\sigma_p}{S_o} = \frac{2R\,(1 - x/5 + h) - kh\,(1 - w + w_p n)}{hn + 1.8(1 - r)(1 + h/(1 - x/5)) + 2Rb(1 - w)/\pi} \qquad \text{Eq. 1}$$

where $\Delta\sigma_p$ is the increase in pillar stress resulting from the mining-out of the adjacent stopes;

S_o is the normal field stress perpendicular to the vein;

R is the extraction ratio;

x $= x'/l$, the dimensionless x-coordinate of the particular pillar;

* These numbers refer to the sources of information listed in the bibliography at the end of this report.

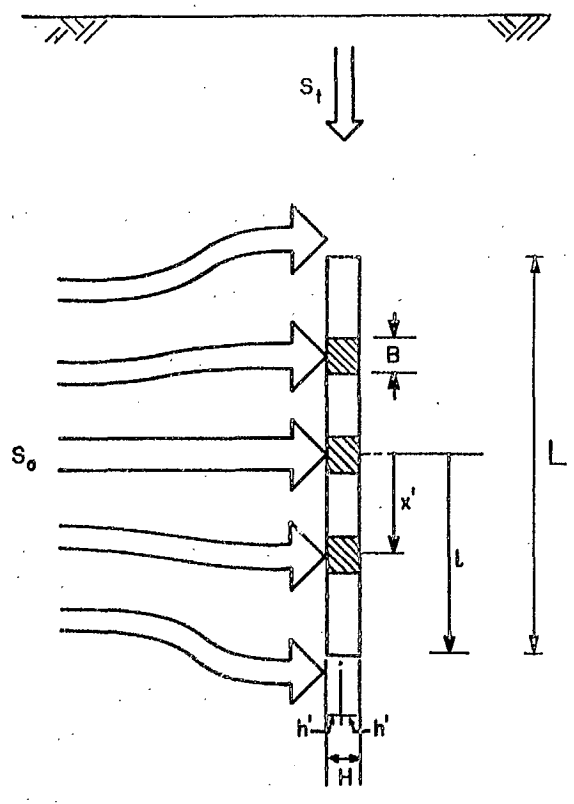

Figure 1. Idealized mining zone containing pillars.

h = h'/l, the dimensionless height of the pillar;

k = S_t/S_o, the ratio of transverse to normal field stress components;

S_t is the field stress parallel to the seam or vein and normal to strike;

w = $\mu/(1-\mu)$, and μ is Poisson's ratio of the wall rock;

w_p is the same parameter for the pillar rock;

n = M/M_p and $M = E/(1-\mu^2)$, with E being the modulus of deformation of the wall rock and M_p being the same parameter for the pillar rock;

r is the local extraction ratio based on the area tributary to the pillar in question;

and b is equal to B/L, the dimensionless pillar width.

Based on the same mechanisms, but recognizing the difference in loading conditions, the appropriate equation to be used in analysing

the model work is as follows:

$$\frac{\sigma_p}{S_o} = \frac{(2+h)(1 - x/5 + h) - kh}{hn + 1.8(1 - r)(1+h/(1 - x/5)) + 2Rb(1 - \mu)/\pi} \quad \text{Eq. 2}$$

After this basic work has been done, it remained to consider the applicability of the hypothesis to the cases of orebodies dipping at angles between 0^o and 90^o, or, more generally, to the cases where the major principal field stress is inclined into the plane of the orebody. A simple application of the hypothesis would be to predict the pillar stresses using only the field stresses normal and transverse to the workings, ignoring the shear stresses parallel to the workings. The theoretical implications of using such an approach are examined below by comparing the deflections that would be obtained for a completely mined-out ore zone, with the theoretical deflections that would be obtained with an elliptical opening using the theory of elasticity.

THEORY

Application of Previous Hypothesis

It has been shown (2) that the hypothesis predicts vertical deflections on the surface of a slot in models according to the following equation:

$$\delta = \frac{S_o\, t}{E}(2+h - kh)((1 - x^2)^{\frac{1}{2}} + h) \quad \text{Eq. 3}$$

Applied to an elliptical hole, this equation would be:

$$\delta = \frac{S_o\, t}{E}(2+h - kh)(1 - x^2)^{\frac{1}{2}},$$

where δ is the vertical direction and the other terms are as previously defined.

For the general case of biaxial stress with the major principal field stress, S_1, at an angle α to the major axis of the ellipse:

$$S_o = S_1 \sin^2 \alpha + S_3 \cos^2 \alpha$$

$$S_t = S_1 \cos^2 \alpha + S_3 \sin^2 \alpha .$$

Since the shear on planes parallel to the orebody as shown in Figure 2(b) is ignored when considering closure, C_h, once S_o and S_t have been determined the equation for C_h is independent of α:

$$C_h = 2\delta = \frac{2S_o t}{E}(2 + h - kh)(1 - x^2)^{\frac{1}{2}} \qquad \text{Eq. 4}$$

Closure from Theory of Elasticity

In terms of plane strain with $S_3 = 0$, N.A. Toews (3) has shown that the deflection in the y-direction of a point on the boundary of an ellipse in an inclined stress field, as shown in Figure 2, is:

$$2G\delta_\theta = \frac{S_1 Q}{4}(d + 1)((1 + m) \sin \theta - 2 \sin(\theta - 2\alpha)),$$

where $G = E/2(1 + \mu)$ is the modulus of rigidity;

$Q = (t + h')/2$;

$m = (1 - h')/(1 + h')$;

$d = (3 - 4\mu)$, an elastic modulus; and

θ = the eccentric angle associated with the point $(x' \; y')$ on the ellipse, as shown in Figure 3.

Converting to plane stress,

$$\delta_\theta = \frac{S_1 t}{E}(\sin \theta - (1 + h) \sin(\theta - 2\alpha))$$

$$= \frac{S_o t}{E \sin^2 \alpha}(\sin \theta - (1 + h) \sin(\theta - 2\alpha)).$$

Now the closure, C_t, will be expressed as the algebraic sum of the deflection at the point defined by θ plus that at the vertically opposite point defined by $-\theta$:

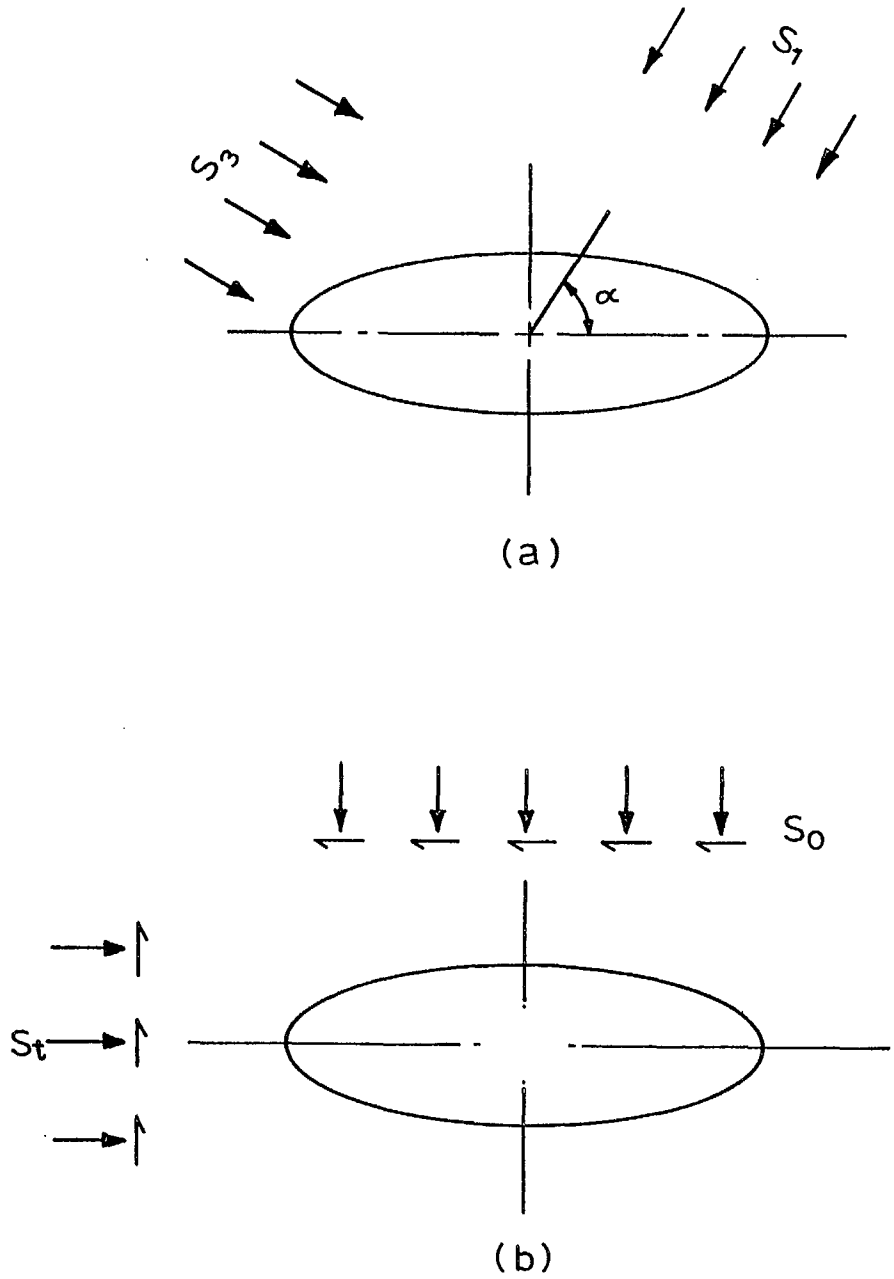

Figure 2. Elliptical hole with axes oblique to the principal field stress directions.

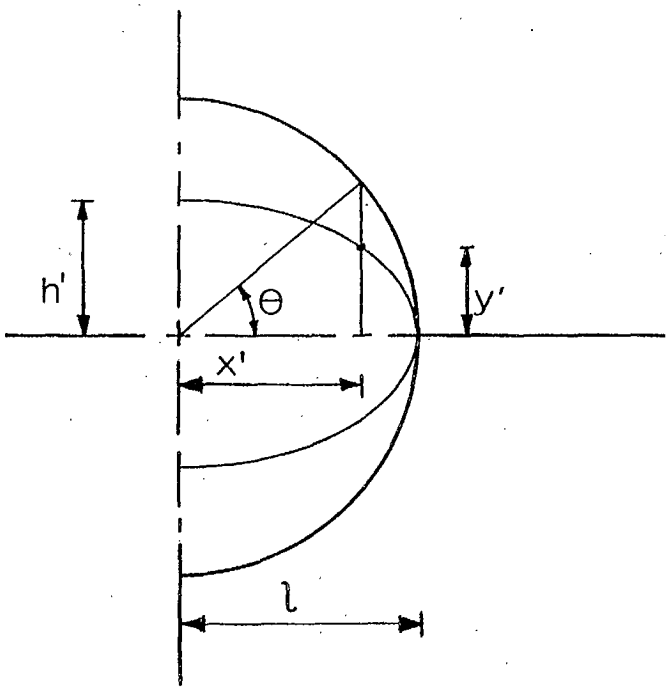

Figure 3. Definition of elliptical coordinates[3].

$$C_t = \delta_\theta - \delta_{-\theta}$$

$$= \frac{S_o l}{E \sin^2 \alpha} (\sin\theta - \sin(-\theta) - (1+h)\sin(\theta - 2\alpha) + (1+h)\sin((-\theta) - 2\alpha)).$$

Then, since $k = \cos^2 \alpha / \sin^2 \alpha$

$$= \frac{2S_o l \sin\theta}{E} (2 + h - kh).$$

Finally, with $\sin^2 \theta = (l^2 - x'^2)/l^2$ and $x = x'/l$, $\sin\theta = (1 - x^2)^{\frac{1}{2}}$

$$\therefore \quad C_t = \frac{2S_o l}{E} (2+h - kh)(1 - x^2)^{\frac{1}{2}} \qquad \text{Eq. 5}$$

The same equation will be obtained when $S_1 = 0$ and $S_3 > 0$.

Comparison of Results from Hypothesis and Theory of Elasticity

It turns out that Equations 4 and 5 are identical. This means that the closure of a slot predicted by the mechanisms incorporated in the hypothesis should be quite accurate for elastic ground.

In the case where less than 100 per cent extraction occurs--or, in other words, pillars exist--the tendency for closure to occur is the primary mechanism leading to the loading of the pillars. This is modified by the reverse deflection resulting from the back pressure of the pillars, which in turn is influenced by the various geometrical and geological variables (such as the span of the mining zone, the height and breadth of the pillar, the position of the pillar in the mining zone, or any difference in deformability between the pillar and wall rock).

At the same time, it cannot be ignored that whereas these conclusions may be valid for the average pillar stresses, the theory of elasticity shows that the deflection of a point on one wall will be different from that of a point on the opposite wall, as well as there being different angles of rotation of the wall lines; hence it is clear that there will be different stress concentrations at the corners of the pillars. Figure 4 shows the results obtained in some photoelastic models (4). However, as we are dealing in this work with the pillar loading, the average stress can be used for this purpose. Later consideration of failure must examine, among other factors, this variation of stress.

EXPERIMENTAL DATA AND ANALYSIS

Model Description and Operation

The series of models in steel plates, used for the initial work, was continued in examining the mechanics of inclined workings (2). Models were constructed out of mild steel plates as shown in Figure 5. The elastic properties of the steel were $E = 30.2 \times 10^6$ psi, and $\mu = 0.290$ (2).

Although in machining the plates a tolerance of 0.002 in. was called for, the actual work was generally done to a tolerance of 0.001 in. In designing the various configurations of pillars and openings, account was taken of the desirability of having the edge distance three times half the span of the mining zone; or, in other words, of the plate's width being four times the entire span of the mining zone, and the cover distance between openings and loaded boundaries being more than 20 times the equivalent radius of the openings.

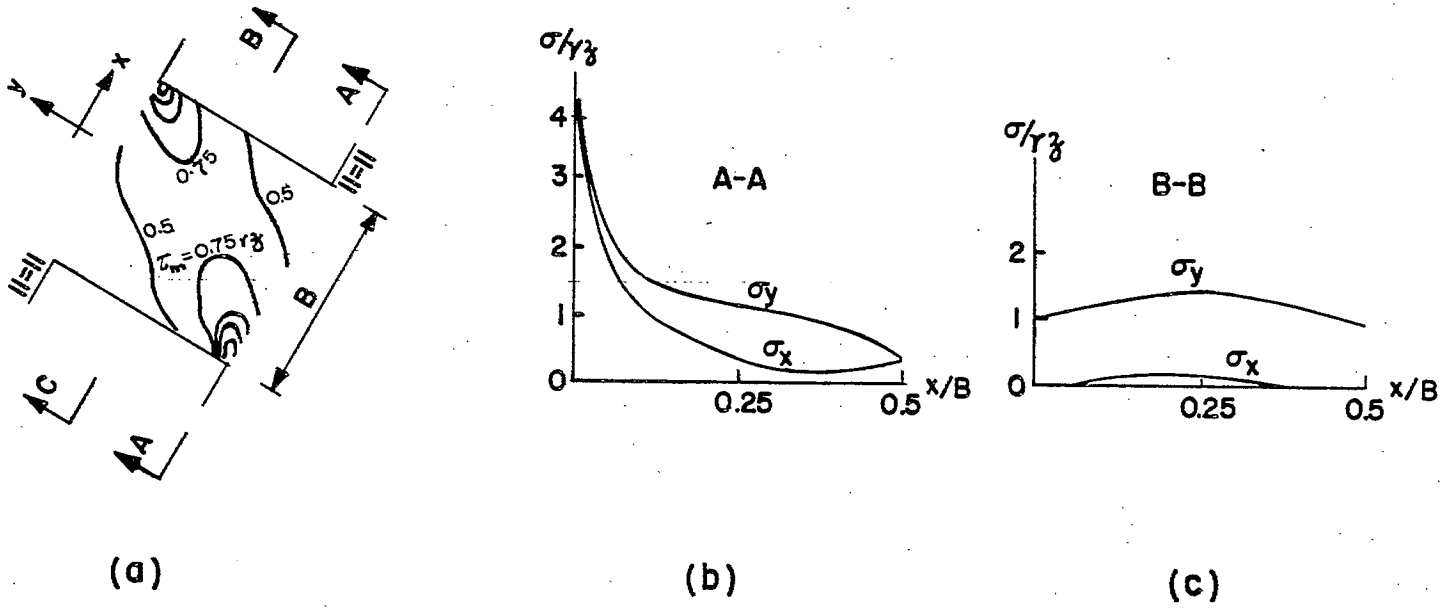

Figure 4. Stress distribution from a gelatin model of a pillar in an inclined mining zone [4].

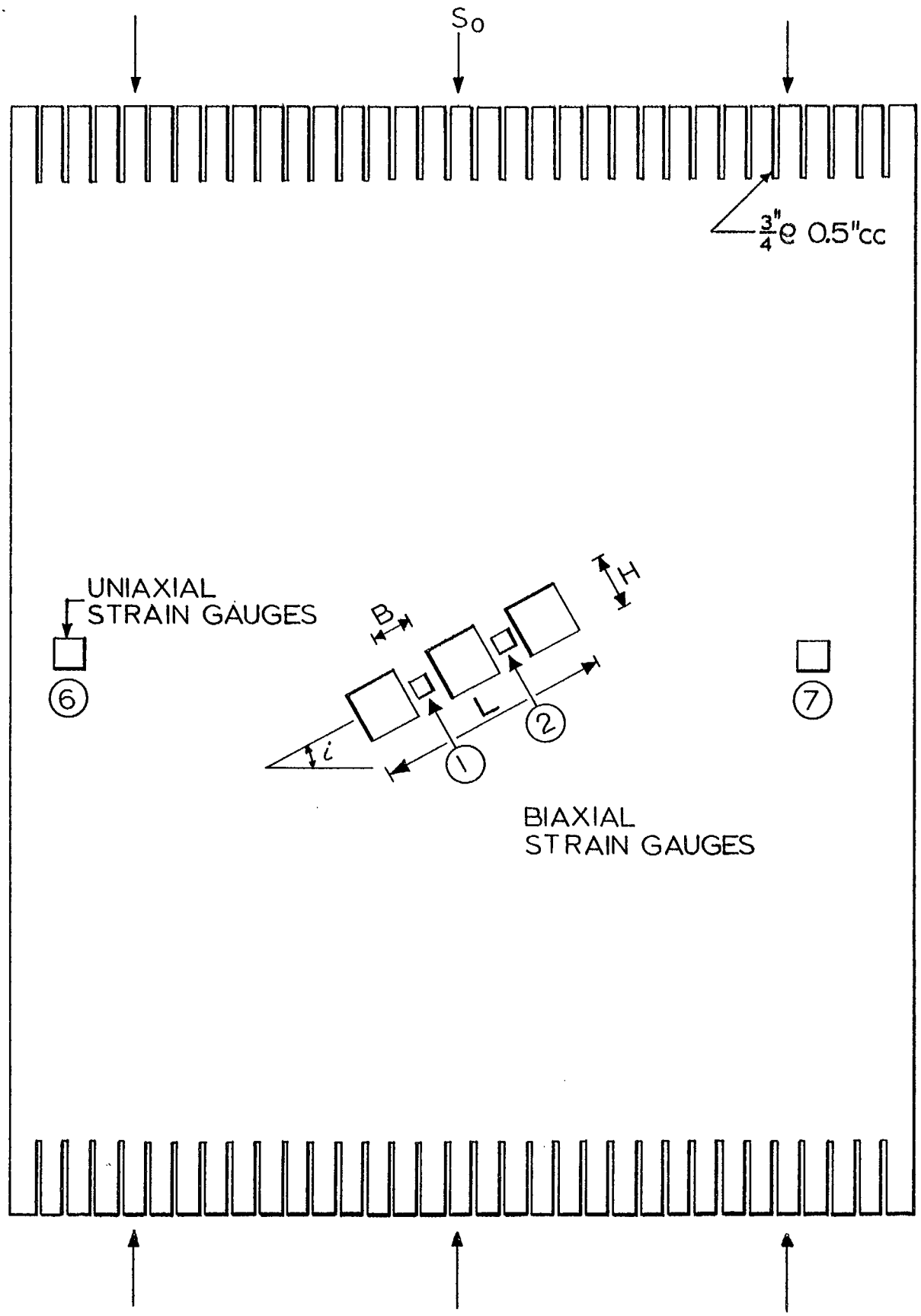

Figure 5. Typical steel plate model of pillars in an inclined mining zone (not to scale).

To simulate the effects of having the compressibility of the pillars greater than that of the wall rocks, plates were constructed with the pillars milled down approximately 0.080 in. on each side.

Biaxial two-element, foil-type strain gauges were used on the pillars to measure both longitudinal and transverse strains. In addition, single-element strain gauges were placed longidutinally on the horizontal centreline of the mining zone at the outer edge of the plate, to provide a comparison with theory of the distribution of the stresses throughout the plate (5) and to check on the magnitude of the loading on the plate. The locations of these gauges, No. 6 and No. 7, are shown in Figure 5.

Gauges were applied to both sides of each pillar and then connected in series so that an average of the two gauges was obtained directly from the single reading. This average compensated for any eccentric loading or slight warping of the plates which might have caused a higher stress on one side than on the other.

To obtain uniform, uniaxial stress in the model plates, a number of devices were used. Strips of lead were placed adjacent to the platens of the testing machine, to eliminate the tendency for stress concentrations to occur towards the sides of the plate. To prevent horizontal stresses from being induced in the plates by the extrusion action on the lead strips, most of the loaded edges had a 1/4-in. thick steel bar placed between the plate and the lead strips. Then, as additional measures to prevent the occurrence of horizontal stresses in the plate, either from extrusion action or from restraint of lateral deflection, two layers of 2-mil Teflon ribbon were placed on the loaded edges of the model plate and, in addition, vertical slots were cut into the plate 3/4 in. deep and spaced 1/2 in. apart. The tests showed that this latter device was particularly effective in eliminating any minor horizontal stress that might otherwise have been induced in the place. Also, to diminish the effects of any remaining end restraint on the models that would be most affected, models S-26, 28, 33 to 36, 38 and 40 were made 20 inches long, whereas the others were only 12 inches long.

After the load on the plate was cycled 2 to 3 times, a zero was set on the bridge for the strain gauges. The plate was then loaded up to 20,000 lb and unloaded, and readings were obtained at 1000, 2000, 6000, 10,000, 16,000 and 20,000 lb. The plate was then turned end for end and a similar series of readings was taken. The readings were then combined into an average and plotted on the graph, using the slope as the strain produced by a unit load on the plate.

Results

Table 1 contains the experimental results, and Figure 6 a typical set of strain curves, obtained from these models.

TABLE 1

Experimental Results
N = 2, μ = 0.290

No.	R	L (in.)	H (in.)	B (in.)	x	k	n	i	σ'_p
S-25	0.749	1.999	0.498	0.251	0.375	0.333	1	30°	2.33
S-26	0.754	2.012	0.500	0.247	0.378	3.00	1	60°	2.21
S-27	0.749	1.999	0.498	0.251	0.375	0.333	1.734	30°	1.95
S-28	0.754	2.012	0.500	0.247	0.378	3.00	1.773	60°	2.21
S-33	0.751	2.000	0.498	0.249	0.375	0.704	1	40°	2.36
S-34	0.751	2.004	0.503	0.250	0.374	1.432	1	50°	2.30
S-35	0.751	2.000	0.498	0.249	0.375	0.704	1.753	40°	1.91
S-36	0.751	2.000	0.498	0.249	0.375	1.432	1.753	50°	1.81
S-37	0.749	1.999	0.500	0.251	0.375	0.133	1	20°	2.42
S-38	0.742	1.990	0.493	0.257	0.377	7.54	1	70°	0.58
S-39	0.749	1.999	0.500	0.251	0.375	0.133	1.732	20°	1.98
S-40	0.742	1.990	0.493	0.257	0.377	7.54	1.750	70°	0.35
S-41	0.754	1.998	0.497	0.253	0.376	0.333	1	30°	2.29
S-42	0.754	1.998	0.497	0.253	0.376	0.333	1.390	30°	2.05
S-43	0.754	2.003	0.498	0.254	0.375	0.704	1	40°	2.35
S-44	0.754	2.003	0.498	0.254	0.375	1.432	1	50°	2.15
S-45	0.754	2.003	0.498	0.254	0.375	0.704	1.405	40°	2.04
S-46	0.754	2.003	0.498	0.254	0.375	1.432	1.405	50°	2.05
S-47	0.748	1.996	0.496	0.251	0.376	0.132	1	20°	2.35
S-48	0.748	1.996	0.496	0.251	0.376	0.132	1.445	20°	2.04
S-49	0.774	2.001	0.502	0.226	0.386	3.00	1	60°	2.04
S-50	0.774	2.001	0.502	0.226	0.386	3.00	1.566	60°	1.84

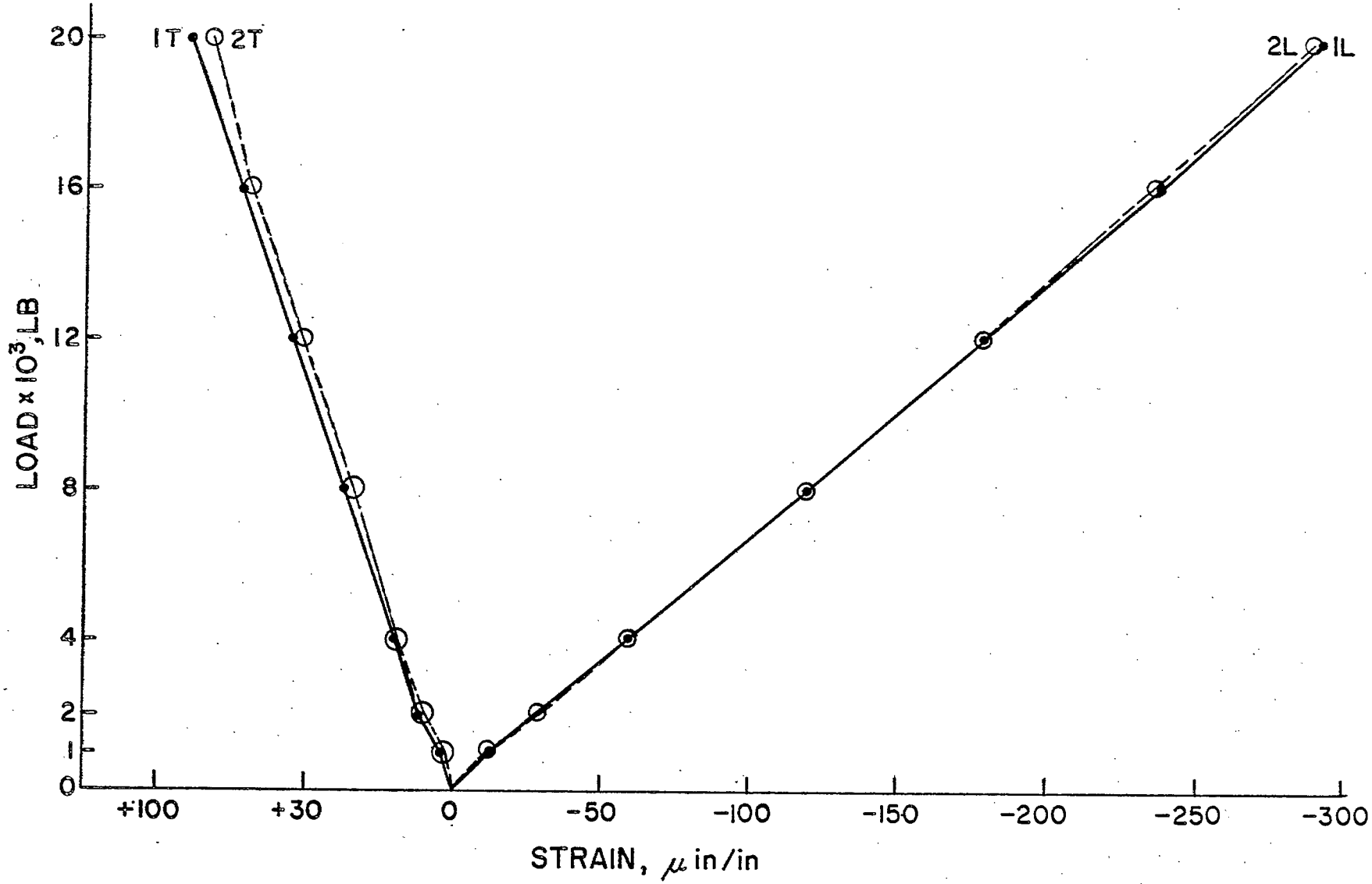

Figure 6. Typical set of strain curves obtained in steel plate model S-36. 1L and 2L are for longitudinal strains in the two pillars, and 1T and 2T for the transverse strains (see Figure 5).

Analysis

The experimental data have been analysed by determining the pillar loading as a function of the field stress normal to the workings and comparing this with the calculated pillar loading, using the hypothesis as expressed by Equation 2. The results of these calculations are shown in Table 2.

TABLE 2

Analysis of Data
$N = 2,\ \mu = 0.290$

No.	R	h	b	x	i	k	n	$\sigma'_{p\ EXPT}$	$\sigma'_{p\ HYP}$	$\frac{EXP}{HYP}$
S-25	0.749	0.249	0.126	0.375	30°	0.333	1	2.33	2.43	0.96
S-26	0.754	0.249	0.123	0.378	60°	3.00	1	2.21	1.82	1.21
S-27	0.749	0.249	0.126	0.375	30°	0.333	1.734	1.95	2.06	0.95
S-28	0.754	0.249	0.123	0.378	60°	3.00	1.773	1.59	1.54	1.03
S-33	0.751	0.249	0.124	0.375	40°	0.705	1	2.36	2.35	1.00
S-34	0.751	0.251	0.125	0.374	50°	1.432	1	2.30	2.17	1.06
S-35	0.751	0.249	0.124	0.375	40°	0.704	1.753	1.91	1.99	0.96
S-36	0.751	0.249	0.124	0.375	50°	1.432	1.753	1.81	1.83	0.99
S-37	0.749	0.250	0.126	0.375	20°	0.133	1	2.42	2.44	0.99
S-38	0.742	0.248	0.129	0.377	70°	7.54	1	0.58	0.69	0.86
S-39	0.749	0.250	0.126	0.375	20°	0.133	1.732	1.98	2.08	0.96
S-40	0.742	0.248	0.129	0.377	70°	7.54	1.750	0.35	0.57	0.62
S-41	0.745	0.250	0.127	0.376	30°	0.333	1	2.29	2.40	0.96
S-42	0.745	0.250	0.127	0.376	30°	0.333	1.390	2.05	2.20	0.93
S-43	0.745	0.248	0.127	0.375	40°	0.704	1	2.35	2.29	1.03
S-44	0.745	0.248	0.127	0.375	50°	1.432	1	2.15	2.12	1.02
S-45	0.745	0.248	0.127	0.375	40°	0.704	1.405	2.04	2.12	0.96
S-46	0.745	0.248	0.127	0.375	50°	1.432	1.405	2.05	1.95	1.05
S-47	0.748	0.249	0.126	0.376	20°	0.132	1	2.35	2.51	0.94
S-48	0.748	0.249	0.126	0.376	20°	0.132	1.445	2.04	2.27	0.90
S-49	0.774	0.251	0.113	0.386	60°	3.00	1	2.04	1.92	1.06
S-50	0.774	0.251	0.113	0.386	60°	3.00	1.566	1.86	1.68	1.09

The dimensionless parameters h, b and x were obtained, as in the previous work (1), by dividing the semi-heights and breadths of the pillars (H/2 and B/2) and the actual x-coordinate, x', from the centreline of the mining zone by the semi-span, L/2. The coefficient k, defined as the ratio of transverse field stress to normal field stress S_t/S_o, varied with the angle of dip:

$$k = (1 - \cos 2i)/(1 + \cos 2i).$$

As was done in the previous work (2), after an initial run the pillars were milled down to a thickness less than that of the plate, to simulate the effect of a lower modulus of elasticity in the pillar than in the wall rock. The ratio of the thickness of the plate to the thickness of the pillar is actually equivalent to n, the ratio of the modulus of deformation of the wall rock to the modulus of the pillar rock.

The pillar loading, σ'_p, for the models was determined by calculating the longitudinal stress in the pillars, taking into account the transverse strain effects, and expressing this as the ratio of the stress in the plate normal to the plane of the workings. The predicted pillar loading by the hypothesis was calculated using Equation 2.

A scatter diagram is shown, in Figure 7, of the ratio of the experimental values to the hypothesis values of pillar loading versus the angle of dip.

The results show that, except for dip angles beyond 50°, the average deviation of the experimental to hypothesis values is less than 5 per cent, which is well within that to be expected when taking into account the magnitudes of the possible experimental errors. At the dip of 60° the normal stress, S_o, is about half the principal stress, S_i, and at 70° S_o is about a quarter of S_i. Hence, the deviations at the high dip angles are particularly sensitive to experimental errors, as the relative strain level in these pillars is low, making the degree of accuracy in the gauges and geometry of particular significance. For example, a 1° error in the dip angle, i, would lead to a 42 per cent error in the ratio EXPT/HYP.

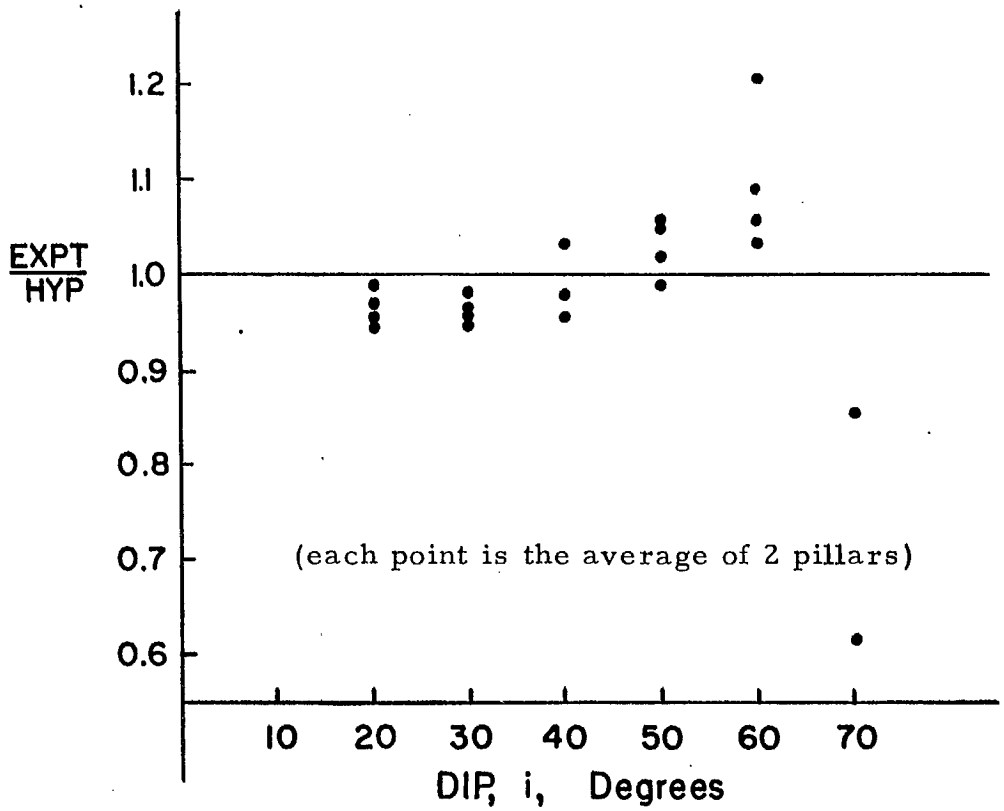

Figure 7. Scatter diagram of the ratio of experimental values (EXPT) to predicted values by the hypothesis (HYP) versus the angle of dip, i.

CONCLUSIONS

The equations produced by the previous work in developing a hypothesis of pillar loading have been shown to provide good predictions for the loading of model pillars in workings at dip angles between 20° and 70°. It is concluded, therefore, that the previously developed Equation 1 for long, deep mining zones can be used for engineering purposes.

Inasmuch as Equation 1 is semi-empirical, its applicability can only be claimed for ranges which are in the various parameters covered by the experimental data. Presumably, some extrapolation would be valid, but there is the danger that any inaccuracies in the functional relations would become more significant for distinctly different ranges of some of the parameters.

The range in the parameter x in the empirical data was from 0 to 0.8, which is substantially the full range that occurs in practice.

The range in values of the parameter h was from 0.08 to 1.3, extending on the high side beyond the normal range but not including mine geometries (where pillar heights could be as small as 0.01 of the semi-span of the mining zone). However, considering how h affects the mechanics of the problem, it is improbable that the range not covered by the experimental data would not be predicted by the hypothesis.

The range in the parameter b in the experimental work extends from 0.01 to 0.43, which probably covers more than the common range of pillar breadths.

The range in values included in the experimental data for the parameter k was previously from 0 to 3, and this current work extends the range up to approximately 7.5. It is unlikely that the actual range in k in the earth's crust would exceed the experimental values; consequently, the hypothesis should be valid for any field stress conditions.

The range in the parameter N in all of this work was from 1 to 8, beyond which N tends to become insignificant. There should, therefore, be no limitation on the use of the hypothesis with respect to this parameter.

The range in the parameter n is from 1 to 1.7. For values of n outside this range, the hypothesis would have to be used with caution.

The extraction ratio R is, of course, the most important parameter governing pillar loading. The range in values covered by the experimental data was from 0.5 to 0.9, substantially covering the full range required for the parameter.

ACKNOWLEDGEMENTS

Great assistance was provided in this work by Mr. J.D. Sullivan in the laboratory and by Miss M. Ellis in the computations. The editing was done with the good services of Mr. P.E. Shannon, Mines Branch.

BIBLIOGRAPHY

1. Coates, D.F., "Pillar Loading. Part I: Literature Survey and New Hypothesis", Mines Branch Research Report R 168, Canada Department of Mines and Technical Surveys, Ottawa (1965).

2. Coates, D.F., "Pillar Loading. Part II: Model Studies", Mines Branch Research Report R 170, Canada Department of Mines and Technical Surveys, Ottawa (1965).

3. Toews, N.A., personal notes (1965).

4. Trumbachev, C. and Melnikov, E., "The Effect of the Dip Angles of a Deposit on the Distribution of Stresses in Interchamber Pillars", Teknologia i Eknomika Ugledobychi, No. 3, Moscow (1961).

5. Howland, R., "On the Stresses in the Neighbourhood of a Circular Hole in a Strip under Tension", Phil. Trans. Roy. Soc. (A), Vol. 229, p. 49 (1929).

- - - -

DFC:(PES)/DV

APPENDIX

GLOSSARY OF ABBREVIATIONS

(Note: After many of the terms, letters in brackets indicate the fundamental dimensions of the physical quantity; e.g., L stands for length, M for mass, F for force, T for time, and S signifies that the quantity is dimensionless.)

$a(L)$	-	radius of a circle or major semi-axis of an ellipse
$A_o(L^2)$	-	total area of walls adjacent to the mined-out rooms or stopes of the entire mining zone
$A_p(L^2)$	-	area of a pillar parallel to the walls
$A_t(L^2)$	-	area of walls tributary to a pillar
$A_T(L^2)$	-	area of walls adjacent to the entire mining zone
$b(D)$	-	width of pillar (B/L)
$b(L)$	-	minor semi-axis of an ellipse
$b_o(D)$	-	width of opening (B_o/L)
$B(L)$	-	width of pillar
$B_o(L)$	-	width of opening (stope or room)
c c(L)	-	centre to centre
$cc(L^3)$	-	cubic centimetre
$cf(L^3)$	-	cubic foot
$c(FL^{-2})$	-	cohesion
$ci(L^3)$	-	cubic inch
cm(L)	-	centimetre
cpn	-	compression
$C_h(L)$	-	closure of the walls of a slot or mining opening with 100 per cent extraction
$C_t(L)$	-	closure of the walls of an elliptical opening determined from the theory of elasticity
$C_b(D)$	-	coefficient of $\frac{WL^3}{EI}$ for calculating the deflection of a beam due to bending moment
$C_s(D)$	-	coefficient of $\frac{WL^3}{EI}$ for calculating the deflection of a beam due to shear force

d(D)	-	parameter of an ellipse $(3 - 4\mu)$ in plane strain and $(3 - \mu)/(1 + \mu)$ in plane stress
dia(l)	-	diameter
Eq.	-	equation
$E(FL^{-2})$	-	modulus of linear deformation (Young's modulus)
$E_p(FL^{-2})$	-	modulus of deformation of pillar rock
ft(L)	-	feet
$F_s(D)$	-	factor of safety
$G(FL^{-2})$	-	modulus of shear deformation
h'(L)	-	semi-height of a pillar
h(D)	-	dimensionless height of a pillar (H/L)
H(L)	-	height of pillar
i(D)	-	angle of dip to horizontal
in.(L)	-	inch
$I(L^4$ or $ML^2)$	-	moment of inertia
k(D)	-	S_t/S_o or σ_h/σ_v
$k_s(L^3F^{-1})$	-	coefficient of subgrade reaction, δ/q
ksc	-	kilograms per square centimetre
l	-	semi-span of a mining zone (L/2)
ln a	-	natural logarithm of a
log a	-	logarithm of a to base 10
LF	-	linear foot
L(L)	-	breadth of mining zone
max	-	maximum

m(D)	-	Poisson's number
m(D)	-	parameter of an ellipse (a-b)/(a+b)
min	-	minimum
$M(FL^{-2})$	-	$E/(1 - \mu^2)$
M(FL)	-	moment
n(D)	-	ratio of moduli of deformation (M/Mp or E/Ep)
N(D)	-	number of pillars
$p(FL^{-2})$	-	contact pressure
$pcf(FL^{-3})$	-	pounds per cubic foot
$psf(FL^{-2})$	-	pounds per square foot
$psi(FL^{-2})$	-	pounds per square inch
P(F)	-	a pillar load
$q(FL^{-2})$	-	bearing pressure
$Q_B(FL^{-2})$	-	uniaxial compressive strength of a sample of width B
$Q_o(FL^{-2})$	-	uniaxial compressive strength for a sample of unit width
$Q_u(FL^{-2})$	-	uniaxial compressive strength
r(D)	-	local extraction ratio, i.e. based on tributary area to single pillar
r(L)	-	radius or radial distance
R(D)	-	extraction ratio (wall area excavated/total wall area); parameter of an ellipse (a+b)/2
R(L)	-	radius or radial distance
$sf(L^2)$	-	square foot

$si(L^2)$ - square inch

$S(L^{-3})$ - section modulus

$S_h(FL^{-2})$ - field stress in the horizontal direction

$S_t(FL^{-2})$ - field stress parallel to the seam or vein and normal to strike

$S_v(FL^{-2})$ - field stress in the vertical direction

$S_o(FL^{-2})$ - field stress normal to seam or vein

$S_p(FL^{-2})$ - average pillar pressure on walls $\Sigma P/\Sigma A_t$

$S_x(FL^{-2})$ - field stress in the x-direction

$S_y(FL^{-2})$ - field stress in the y-direction

$S_z(FL^{-2})$ - field stress in the z-direction

tsn - tension

TA - tributary area

$v_r(L)$ - radial displacement

$v_\theta(L)$ - tangential displacement

V(F) - shear force

w(D) - $\mu/(1-\mu)$

wrt - with respect to

$W(F \text{ or } MLT^{-2})$ - load or weight

x(L or D) - linear displacement or coordinate or dimensionless distance (x'/ℓ) in direction of x-axis

x'(L) - linear displacement or coordinate in direction of x-axis

y'(L) - linear displacement or coordinate in direction of y-axis

$\delta(L)$	-	inward displacement of wall normal to vein or seam; or just displacement
$\delta'(L)$	-	reverse displacement of wall due to average pillar pressure
$\delta A(L)$	-	abutment compression or deformation
$\delta_c(L)$	-	displacement of wall normal to vein or seam at centreline
$\delta_e(L)$	-	inward displacement of wall normal to vein (or seam), resulting from excavation of stopes or rooms
$\delta'_p(L)$	-	local penetration of a pillar into the wall
$\delta_x(L)$	-	displacement of wall normal to vein or seam at x from centreline
$\gamma(D)$	-	shear strain
$\gamma(FL^{-3})$	-	unit weight (bulk density)
$\epsilon(D)$	-	linear strain
$\epsilon_r(D)$	-	linear strain in the radial direction
$\epsilon_t(D)$	-	linear strain in the tangential direction
$\epsilon_\theta(D)$	-	linear strain in the tangential direction
$\mu(D)$	-	Poisson's ratio
$\rho(L)$	-	radius of curvature
$\sigma(FL^{-2})$	-	normal stress
$\sigma_p(FL^{-2})$	-	pillar stress P/A_p
$\bar{\sigma}_p'(D)$	-	σ_p/S_o
$\sigma_p(FL^{-2})$	-	average pillar stress $\Sigma P/\Sigma A_p$
$\Delta\sigma_p(FL^{-2})'$	-	increase in pillar stress due to mining

$\Delta\sigma_p'(D)$ - $\Delta\sigma_p/S_o$

$\sigma_r(FL^{-2})$ - radial stress

$\sigma_\theta(FL^{-2})$ - tangential stress

$\sigma_t(FL^{-2})$ - tangential stress

$\sigma_1(FL^{-2})$ - major principal stress

$\sigma_2(FL^{-2})$ - intermediate principal stress

$\sigma_3(FL^{-2})$ - minor principal stress

$\tau(FL^{-2})$ - shear stress

- - - -